eNeuro Accepted Manuscript

eNeuro

Research Article: New Research | Cognition and Behavior

miR-92a Suppresses Mushroom Body-Dependent Memory Consolidation in *Drosophila*

https://doi.org/10.1523/ENEURO.0224-20.2020

Cite as: eNeuro 2020; 10.1523/ENEURO.0224-20.2020

Received: 26 May 2020
Revised: 28 July 2020
Accepted: 28 July 2020

This Early Release article has been peer-reviewed and accepted, but has not been through the composition and copyediting processes. The final version may differ slightly in style or formatting and will contain links to any extended data.

Alerts: Sign up at www.eneuro.org/alerts to receive customized email alerts when the fully formatted version of this article is published.

Copyright © 2020 Guven-Ozkan et al.
This is an open-access article distributed under the terms of the Creative Commons Attribution 4.0 International license, which permits unrestricted use, distribution and reproduction in any medium provided that the original work is properly attributed.

eNeuro Accepted Manuscript

1. Manuscript Title

miR-92a Suppresses Mushroom Body-Dependent Memory Consolidation in *Drosophila*

2. Abbreviated Title (50 character maximum)

microRNA function in memory suppression

3. List all Author Names and Affiliations in order as they would appear in the published article

Tugba Guven-Ozkan[1], Germain U. Busto[1,2], Jae-Yoon Jung[3], Ilaria Drago[1], Ronald L. Davis[1]*

[1]Department of Neuroscience

The Scripps Research Institute Florida

Jupiter, FL 33458, USA

[2] Current Address: Genetics & Development Department

Institute of Human Genetics

Montpellier 34396, France

[3]Department of Pediatrics/Systems Medicine

Stanford University

Stanford, CA 94305, USA

4. Author Contributions:

eNeuro Accepted Manuscript

TGO and RLD designed the specific experiments and TG performed most them. ID helped with *R28H05>miR-92a* behavior experiments. GB provided assistance at a broader level of our microRNA project. David Van Vactor, Dennis Wall, and Jae-Yoon Jung designed and implemented the target gene identification pipeline. TGO and RLD wrote the initial draft of the manuscript that was then edited by all authors.

5. Correspondence should be addressed to (include email address)

Ronald L. Davis

Department of Neuroscience

The Scripps Research Institute Florida

Jupiter, FL 33458, USA

email: rdavis@scripps.edu

6. Number of Figures

10

7. Number of Tables

1

8. Number of Multimedia

NA

9. Number of words for Abstract

138

10. Number of words for Significance Statement

eNeuro Accepted Manuscript

78

11. Number of words for Introduction

484

12. Number of words for Discussion

1256

13. Acknowledgements

We would like to acknowledge David Van Vactor (Harvard) and Tudor Fulga (Oxford) for the *miRNA* sponge lines; Seth Tomchik (Scripps) for *D2R* mutant stock. We also thank Pejmun Haghighi (Buck), Fen-Biao Gao (UMass), Chris Doe (U Oregon), the Vienna Drosophila RNAi Center (VDRC), and the Bloomington *Drosophila* Stock Center for other fly lines. The project was assisted by the Bioinformatics Core of P01 NS090994; David Van Vactor (PI) and Dennis Wall (Core Director). We appreciate their assistance. We are grateful to Courtney M. MacMullen for technical support.

14. Conflict of Interest

No. Authors report no conflict of interest

15. Funding sources

This research was supported by NIH grants 1R35NS097224 to RLD and 1P01NS090994 and DVV.

eNeuro Accepted Manuscript

ABSTRACT

MicroRNAs fine tune gene expression to regulate many aspects of nervous system physiology. Here, we show that *miR-92a* suppresses memory consolidation that occurs in the αβ and γ mushroom body neurons of *Drosophila*, making *miR-92a* a memory suppressor microRNA. Bioinformatics analyses suggested that mRNAs encoding kinesin heavy chain 73 (Khc73), a protein that belongs to Kinesin-3 family of anterograde motor proteins, may be a functional target of *miR-92a.* Behavioral studies that employed expression of *khc73* with and without its 3'UTR containing *miR-92a* target sites, luciferase assays in HEK cells with reporters containing wild-type and mutant target sequences in the *khc73* 3' UTR, and immunohistochemistry experiments involving Khc73 expression with and without the wild-type *khc73* 3'UTR all point to the conclusion that *khc73* is a major target of *miR-92a* in its functional role as a microRNA memory suppressor gene.

SIGNIFICANCE STATEMENT

Much remains to be learned about how microRNAs regulate gene expression for cognitive processes such as memory formation. The important questions include which of the many different microRNAs are involved, what are their targets, and what specific aspects of memory formation do they regulate? Here we show that the microRNA, miR-92a, normally functions to suppress the consolidation of memories by repressing the expression of a specific kinesin molecule, khc73, in the mushroom body neurons of the Drosophila brain.

eNeuro Accepted Manuscript

KEYWORDS

Memory consolidation, memory suppressor gene, microRNA, kinesin heavy chain

INTRODUCTION

MicroRNAs (miRNAs) are small non-coding RNAs that regulate gene repression post-transcriptionally. Since their discovery less than two decades ago, miRNAs have been implicated in diverse biological processes and diseases. The *miR-17-92* cluster in humans was one of the earliest miRNAs discovered. It is overexpressed in certain types of cancer and thus named, *oncomiR-1* (He et al., 2005). In addition to its function as an oncogene, this cluster of miRNAs has been implicated in development, immune disease, neurodegenerative diseases and aging (Mogilyansky and Rigoutsos, 2013). The nervous system functions of *miR-17-92* cluster include the regulation of axonal outgrowth in embryonic cortical neurons (Zhang et al., 2013), hippocampal neurogenesis, and modulation of anxiety, depressive-like behavior, and pain in response to nerve injury in adult rodent models (Jin et al., 2016; Sakai et al., 2017).

Six miRNAs comprise the *miR-17-92* cluster, with the functions of individual miRNAs in the cluster generally remaining unclear. However, one miRNA in the cluster, *miR-92a,* regulates neuronal progenitor cell divisions and differentiation during the development of the mouse embryonic neocortex and division of *Drosophila* neuroblasts (Bian et al., 2013; Yuva-Aydemir et al., 2015), suggesting conservation of function. A role for *miR-92a* in homeostatic synaptic scaling by repressing rat hippocampal GluA1 subunits of AMPA receptors has been reported (Letellier et al., 2014). In addition, the levels of *miR-*

eNeuro Accepted Manuscript

107 *92a* cycle in adult *Drosophila* PDF (pigment-dispersing factor) neurons across day and
108 night, thus underlying the rhythmicity in excitability of these neurons (Chen and
109 Rosbash, 2017).
110
111 Here, we show that *miR-92a* suppresses *Drosophila* olfactory memory consolidation by
112 constraining the expression of kinesin *heavy chain 73 (khc73)*. *khc73* is homologous to
113 the mammalian *Kif13b/GAKIN/*Kinesin-3 family of proteins that have plus end-directed
114 microtubule motor activity. *khc73* is expressed specifically in the nervous system by late
115 stages of *Drosophila* embryogenesis (Li et al., 1997) and has a role in asymmetric
116 neuroblast division (Siegrist and Doe, 2005). Kinesin family members also participate in
117 the transport of cargo in axons (Horiguchi et al., 2006), maturation of presynaptic
118 release sites and synaptic function (Tsurudome et al., 2010).
119
120 Since restricting *miR-92a* expression enhances memory consolidation, its normal
121 function must be to suppress consolidation. Hence, *miR-92a* is characterized as a
122 memory suppressor gene, which we define as any gene that enhances memory
123 performance when removed functionally from an organism. We show that the memory
124 suppressor function is specific to a form of consolidated memory named anesthesia
125 resistant memory (ARM), and that this suppressing function maps to the $\alpha\beta$ and γ
126 mushroom body neurons (MBn) – neurons known to have dominant roles in olfactory
127 memory formation (Guven-Ozkan and Davis, 2014; Heisenberg, 2003). Opposite to
128 *miR-92a,* we identify *khc73* as a memory promoting gene, enhancing memory
129 consolidation when overexpressed. We present other results showing that *khc73* is a

eNeuro Accepted Manuscript

target of *miR-92a*. From a broader perspective, our results indicate that memory consolidation requires anterograde motor proteins, presumably by transporting synaptic cargo from the soma to synapses mediating consolidation.

MATERIALS AND METHODS

Fly Stocks

Flies were cultured using standard methods. The flies used for *miR-92a* inhibition *(UAS-miR92aSP)* contained two copies of the sponge transgene, one copy on the second chromosome and another on the third. Similarly, the *UAS-scrambled* control flies carried a double insertion of the transgene on chromosomes 2 and 3 (Loya et al., 2009; Fulga et al., 2015). *miR-92a* genomic deletions were as described (Yuva-Aydemir et al., 2015). Other *UAS* transgenic lines included *UAS-miR-92a* (Yuva-Aydemir et al., 2015), *UAS-khc73, UAS-HA-khc73* (Siegrist and Doe, 2005), *UAS-HA-khc73+*$^{3'UTR}$ (Tsurudome et al., 2010), VDRC RNAi lines and *UAS-dcr-2* (Dietzl et al., 2007). *GAL4* lines used include *1471, c155*, *c305a, c739, Gad, GH146, MB-GeneSwitch (247-GeneSwitch), MZ604*, *nSyb, R11D09, R13F02*, *R25H11, R28H05, R35B12, Repo, TH*, *VT64246*.

Behavior

One- to 5-day-old flies were used for standard two-odor discriminative aversive conditioning paradigm (Beck et al., 2000; Busto et al., 2015; Guven-Ozkan et al., 2016). The odorants used were benzaldehyde (ben) and 3-octanol (oct). Memory was tested using a T-maze. For ARM experiments, anesthesia was induced at different time points after conditioning by transferring flies to glass vials and keeping them on ice for 2 min

eNeuro Accepted Manuscript

followed by recovery in regular food vials. For Gene Switch experiments, flies were fed on food containing 200μM RU486 (Mifepristone-Sigma) to regulate *UAS*-driven transgene expression. Memory retention, acquisition, odor and shock avoidance experiments were performed as described (Busto et al., 2015; Guven-Ozkan et al., 2016).

Bioinformatics and statistical analyses

Putative mRNA targets for *miR-92a* were predicted using online tools DIANA-microT-CDS (Paraskevopoulou et al., 2013), TargetScan (Lewis et al., 2005; Ruby et al., 2007) and miRecords (Xiao et al., 2009). The pipeline was designed to select the candidate genes with strong prediction by multiple algorithms. Human *miR-92a* target genes with homology to *Drosophila* targets were selected using DIOPT (Hu et al., 2011). Graphpad Prism was used for statistical analyses. Two sample, two-tailed Student's t-tests were used to compare two conditions. For multiple group comparisons, one-way ANOVA followed by Dunnett's or Bonferroni's *post-hoc* tests were used.

Molecular Cloning and Mutagenesis

To generate *khc73* luciferase reporter, ~2.7kb of 3'UTR was PCR amplified from *UAS-khc73*$^{+3'UTR}$ genomic DNA and cloned into *psiCheck2* vector downstream of *Renilla luciferase* using the In-Fusion enzyme from Clontech. Three *miR-92a* sites were mutagenized sequentially to generate the triple mutant with an ATAAGCT sequence substituted to GCGGTAC. The triple mutant served as a negative control for *miR-92a* and *miR-310* repression.

eNeuro Accepted Manuscript

176

177 ***Luciferase Assay***

178 HEK293T cells were seeded into 96-well microtiter plates 16h before transfection. 400ng of
179 wild-type or triple mutant *psiCheck2-khc73 3'UTR* constructs were transfected using Qiagen
180 PolyFect Transfection Reagent and a final concentration of 500nM of the miRNA mimic
181 (Dharmacon). *Drosophila miR-310* served as positive and *C. elegans miR-239b* as negative
182 controls. Luciferase substrate of the Dual-Glo Luciferase Assay System (Promega) was used
183 to activate Firefly signal followed by Stop&Glo substrate to inhibit Firefly and activate Renilla
184 subsequently. A CLARIOstar plate reader from BMG Labtech was used to measure Firefly and
185 Renilla luminescence. Renilla luciferase activity was normalized to Firefly. Renilla/Firefly ratios
186 for *miR-92a* and *miR-310* transfections were normalized to the *miR-239b* negative control for
187 both wild-type and triple mutant reporters, independently.

188

189 ***Immunohistochemistry***

190 We followed the protocol described earlier except that we incubated tissue with primary
191 antibodies for 2 days (Cervantes-Sandoval et al., 2016; Guven-Ozkan et al., 2016). The
192 primary antibodies used were mouse anti-HA (1:500, 16B12 Thermofisher) and rabbit
193 anti-Scribble (1:500, Cervantes-Sandoval et al., 2016). Secondary antibodies include
194 Alexa Fluor 488 goat anti-mouse (1:500) and 633 goat anti-rabbit (1:500). Images were
195 obtained using Leica TCS SP8 confocal microscope. Regions of interest (ROI) were
196 defined around MB horizontal lobes or antennal lobes. Mean signal intensities of
197 maximum projection images for 8 Z-sections (3µm each) encompassing the
198 anterior/posterior extent of the MBs were measured using ImageJ. Signal from the

eNeuro Accepted Manuscript

antennal lobes was subtracted from MB signal for background normalization. Ratios of HA and Scribble signals were calculated to minimize brain-to-brain variability. Two sample, two-tailed Student's t-tests were used to compare *scrambled* to *miR-92aSP* brains.

RESULTS

miR-92a inhibition enhances aversive olfactory memory

Employing microRNA (miRNA) sponge transgenes offers a versatile approach to inhibit miRNAs in a time and cell specific manner. We previously screened a large collection of *Drosophila* miRNA sponge transgenic lines for aversive olfactory memory using the pan-neuronal driver, *c155-GAL4* (Busto et al., 2015; Busto et al., 2016; Busto et al., 2017; Guven-Ozkan et al., 2016). Our primary screen identified *miR-92a* as a memory suppressor miRNA since we observed elevated memory performance upon reducing the expression of *miR-92a* with two independent *UAS-miR-92a sponge* transgenes *(miR-92aSP)*. However, further tests failed to consistently reproduce these initial effects (Busto et al., 2015). We reasoned that this variability might be due to weak inhibition, so we tested the effect of expressing two copies of *miR-92aSP* with the *c155-GAL4* driver. The double sponge caused a significant increase in 3hr memory compared to *c155>scrambled* control flies (Figure 1A). To confirm that the memory enhancing effects of expressing *miR-92aSP* are due to reducing *miR-92a* expression, we tested heterozygous adult *miR-92a* knockout flies to mimic the hypomorphic effects of *miR-92aSP* knockdown (Figure 1B). We backcrossed two *miR-92a* knockout lines (named D and N; Yuva-Aydemir et al., 2015) into a *wCS10* background and employed *wCS10* flies

eNeuro Accepted Manuscript

as control. Both D and N clones of the *miR-92a+/-* heterozygotes showed significantly enhanced memory, similar to that observed with *miR-92a sponge (miR-92aSP)* flies. Neither *miR-92aSP* animals, nor *miR-92a+/-* heterozygotes exhibited changes in odor and shock avoidance compared to their respective controls (Figure 1-1).

miR-92a functions in MB αβ and γ neurons during development and adulthood

To delineate the subset of neurons in which *miR-92a* functions as a memory suppressor, we crossed *miR-92aSP* flies with a battery of *GAL4* drivers expressed in different neurons of the olfactory nervous system (Guven-Ozkan and Davis, 2014). We also included a glia specific *GAL4* driver, *Repo-GAL4*. Among all the drivers tested, inhibition of *miR-92a* in MBn using *R13F02-GAL4* resulted in a memory performance that was significantly elevated compared to the respective *scrambled* control (Figure 2A), without altering shock or odor perception (Figure 2-1A). MBn can be classified into three main subtypes based on the trajectory of their axons. Axons of MB αβ and α'β' neurons bifurcate to form both vertical and horizontal branches whereas γ neurons have only a horizontal branch (Crittenden et al., 1998). We used two independent drivers for each MB subtype to inhibit *miR-92a* in a neuron subtype-specific manner (Figure 2B) along with *R13F02-GAL4* for pan-MBn expression. Inhibiting *miR-92a* in MB αβ and γ neurons enhanced memory significantly using *1471-GAL4* and *R11D09-GAL4* for γ neurons, and *c739-GAL4* and *R28H05-GAL4* for αβ neurons (Figure 2B) without altering odor or shock avoidance (Figure 2-1B, C). *R25H11-GAL4,* expressed in both γ and αβ neurons, produced the same memory enhancing effect, further strengthening this observation (Figure 2B, Figure 2-1D). In contrast, *miR-92aSP* expression in α'β'

eNeuro Accepted Manuscript

MBn was without effect (Figure 2B). To test the effect of increasing *miR-92a* expression in γ and αβ MBn, we crossed a *UAS-miR-92a* overexpressing transgene with *R25H11-GAL4.* This genotype exhibited memory performance at the same level as *UAS*- and *GAL4*-only controls (Figure 2C), indicating that *miR-92a* is expressed at saturating levels in control flies for memory phenotypes.

We chose to use the Gene-Switch System to dial *miR-92aSP* expression up or down in MBn at different stages of development (McGuire et al., 2004) to delineate developmental vs adult roles. A MBn-specific Gene-Switch *GAL4* was crossed to *miR92aSP* flies and the progeny were fed the ligand RU486 at different stages to activate the Gene-Switch *GAL4*. Flies raised on RU486-laced food throughout the lifespan served as a positive control while flies raised on non-supplemented food served as negative control (Figure 2D). Surprisingly, *miR-92a* inhibition during development or only during adulthood enhanced 3hr olfactory memory in adult flies compared to flies expressing *scrambled* sequences. We also tested *miR-92SP* memory effect using TARGET system attempting to strengthen our conclusion (McGuire et al., 2004). However, the *GAL4* drivers used, in general, failed to reproduce the memory phenotype even when the animals were kept at 30°C during both developmental and adult stages (data not shown). The reason for this failure is unknown, although it is possible that the drivers employed were simply not strong enough to overcome the repressive effects of *GAL80^{ts}* at the permissive temperature of 30°C.

miR-92a inhibition enhances intermediate-term memory

eNeuro Accepted Manuscript

We tested the memory of *miR-92aSP* flies at different times after aversive conditioning to dissect the phase of memory enhanced by *miR-92a* inhibition. Memory was not altered at 3 min or 1hr after conditioning using the pan-MBn driver *R13F02-GAL4* but was enhanced, relative to control flies, at 2 and 3hr after conditioning. This enhancement disappeared by 6hr (Figure 3A). We replicated and refined this observation by performing the same time course experiment (Figure 3-1A) with drivers that promote expression in the γ (*R11D09)* and the αβ neurons *(R28H05).* These experiments reveal clearly that *miR-92a* inhibition enhances memory at intermediate time points. To further exclude a possible role for *miR-92aSP* in memory immediately after conditioning, hidden by a ceiling effect, we tested 3 min memory performance after training flies with varying numbers of shock pulses to titrate training intensity (Figure 3B, 3-1B). Although performance increased with an increasing number of shock pulses, there was no difference in performance scores between the control and experimental genotype using all three *GAL4* drivers (Figure 3B, 3-1B). These data lead to the strong conclusion that *miR-92a* inhibition enhances intermediate-term memory without effect on memory acquisition.

miR-92a inhibition enhances memory consolidation

To further dissect the intermediate-term memory phenotype, we tested whether *miR-92a* might have a role in memory consolidation. One type of consolidated memory in flies is termed Anesthesia Resistant Memory (ARM; Tempel et al., 1983; Quinn and Dudai, 1976), traditionally studied by subjecting flies to a 2 min cold shock to trigger amnesia after training and remove Anesthesia Sensitive Memory (ASM). The memory

eNeuro Accepted Manuscript

remaining after this insult is then measured at later time points. We measured 3hr memory of *R25H11>miR-92aSP* flies with or without cold shock given at 2hr after training. Interestingly, *miR-92a* inhibition enhanced ARM compared to the *scrambled* control flies indicating a role for *miR-92a* in consolidation of this form of memory (Figure 4A). We reproduced and extended this conclusion by assaying ARM in two other genotypes that express *miR-92aSP* in the γ and the αβ neurons (Figure 3-1C). Moreover, we studied the time course of ARM enhancement by applying the cold shock at various times after training with testing occurring at 3hr. No ARM enhancement was observed with cold shock at 3 or 30 min after training, but cold shock at 1 or 2hr provided the maximal enhancement of ARM (Figure 4B). This indicates that *miR-92a* disruption impacts memory consolidation processes that occur between 30-120 min after conditioning.

miR-92a* target prediction pipeline identifies *khc73* as a potential mRNA target of *miR-92a

To identify *miR-92a* target mRNAs and their possible roles in memory consolidation, we first utilized computational prediction software packages including DIANA-microT-CDS, Targetscan, and miRecords (Lewis et al., 2005; Paraskevopoulou et al., 2013; Ruby et al., 2007; Xiao et al., 2009). To extract the strongest predictions and most likely relevant and conserved targets from among the hundreds predicted by each tool, we employed a stringent pipeline that used all three tools (Figure 5A). DIANA-microT-CDS ranks predicted genes based on an miTG score with the highest score being 1.0. Thirty-three genes were predicted by this tool with a miTG score of 1.0. TargetScan ranks its predictions based on the number of miRNA sites and also on the degree of seed

eNeuro Accepted Manuscript

315 sequence complementarity to predicted sites. We selected 31 genes with at least two
316 predicted *miR-92a* binding sites using this tool. Eleven genes were identified in common
317 using these two different algorithms (Figure 5A). We then determined whether these 11
318 common genes were predicted by miRecords, which reduced the number of genes of
319 interest to 6. (Figure 5A). We identified human homologs of predicted *Drosophila* target
320 genes using DIOPT (Hu et al., 2011) and checked whether their mRNA sequences
321 possessed a 5 or 6 nucleotide match to the human *miR-92a* seed sequence. Finally, the
322 five final genes that showed this possible conservation of *miR*:target interaction in
323 humans were tested to see whether they participated in memory formation by
324 *RNAi* knockdown using a pan-neuronal *nSyb-GAL4* driver (Table S1). The top gene
325 identified by this pipeline, identified from impaired memory scores, was kinesin heavy
326 chain gene, *khc73* (Figure 5B). The impaired memory with RNAi knockdown of *khc73* is
327 opposite of the memory phenotype observed upon expressing *miR-92aSP*, which is
328 expected, given that reducing the *miRNA* repressor should increase *khc73* expression.
329
330 The hypothesis that *khc73* is a target of *miR-92a* predicts that overexpression of khc73
331 should enhance memory, mimicking the memory performance of flies with reduced *miR-*
332 *92a* levels. Consistent with the prediction, we found that *UAS-khc73* overexpression in
333 αβ and γ MBn using *R25H11-GAL4* increased memory performance compared to *UAS-*
334 only and *GAL4*-only controls (Figure 5C), with shock- and odor-avoidance controls
335 failing to explain this enhancement (Figure 2-1E). We made two additional observations
336 from behavioral experiments that provide very significant support for this hypothesis.
337 First, the overexpression of *khc73* in αβ and γ MBn enhanced the same form of memory

eNeuro Accepted Manuscript

338 – ARM – as expression of *miR-92aSP* (Figure 5D). Since there are very few known
339 genetic insults that enhance ARM, the probability that this represents independent
340 processes is extremely small. Second, we overexpressed *UAS-khc73* using the MB-
341 Gene-Switch driver and discovered that increasing *khc73* expression during both
342 developmental and adult stages enhances 3hr memory (Figure 5E). The developmental
343 co-mapping of *khc73* overexpression and *miR-92a* inhibition provides compelling
344 behavioral support for the hypothesis that *khc73* is a primary target of *miR-92a* largely
345 responsible for its memory suppressor function.
346
347 **The *khc73* 3'UTR and *miR-92a* binding sites are critical for function**
348 MiRNAs regulate gene expression post-transcriptionally by binding to sequences in the
349 target gene mRNAs. These binding sites are most often located in the 3' untranslated
350 region (UTR) of the mRNAs (Miura et al., 2014). Target site identification software
351 predicts three potential *miR-92a* binding sites in the *khc73* 3'UTR (Figure 6A). We first
352 tested the relevance of the *khc73* 3'UTR to behavior by comparing memory
353 performance of flies that overexpress *khc73* from previously characterized transgenes
354 that include the normal 2.9 kb *khc73* 3'UTR and those that include only the 3'UTR from
355 SV40 with its polyA sequences (Siegrist and Doe, 2005; Tsurudome et al., 2010).
356 Strikingly, memory performance was significantly enhanced when *khc73* was
357 overexpressed with the SV40 3'UTR, but not when overexpressed with the endogenous
358 2.9kb 3'UTR (Figure 6B). These results support the idea that the *khc73* 3'UTR provides
359 repressive activity to the memory phenotype and is consistent with the hypothesis that
360 *khc73* expression is repressed by *miR-92a*. To determine if *khc73* is a direct target for

eNeuro Accepted Manuscript

361 *miR-92a* in vitro, we generated a 3'UTR dual luciferase reporter with *khc73* 3'UTR using
362 the *psiCheck2* vector. The wildtype *khc73* 3'UTR was cloned downstream of Renilla
363 luciferase so that expression levels may be controlled by regulatory elements present in
364 the *khc73* 3'UTR (Figure 6A). The *psiCheck2* vector also contains a constitutively
365 expressed Firefly luciferase to normalize for transfection efficiency. When the *khc73*
366 3'UTR-reporter vector was co-transfected with *miR-92a RNA mimic* – a chemically
367 synthesized miRNA – into HEK293T cells, the Renilla/Firefly luminescence ratio was
368 significantly reduced compared to a *control mimic* (Figure 6C). Previous studies
369 reported that *khc73* 3'UTR is repressed at the *Drosophila* NMJ by the *miR-310-313*
370 cluster of miRNAs which belong to the same family of miRNAs as *miR-92a* (Tsurudome
371 et al., 2010). We thus used one member of the *miR-310* cluster as positive control and
372 found that co-transfecting *miR-310 mimic* resulted in a similar level of repression as
373 *miR-92a* using the *khc73* 3'UTR reporter. To further expand these results and map the
374 repression effects to the *miR-92a* target sequences in the *khc73* 3'UTR, we generated a
375 mutant luciferase reporter construct, mutating the seed sequences of all three *miR-*
376 *92a/miR-310* sites in the 3'UTR (Figure 6A). The repressive activity observed with *miR-*
377 *92a* and *miR-310* mimics was not observed using the mutant *khc73* 3'UTR construct,
378 strongly indicating that *miR-92a* repression occurs through the *miR-92a* target sites
379 (Figure 6C). We conclude from our luciferase reporter experiments using cultured cells
380 that *miR-92a* targets sequences in the wild-type *khc73* 3'UTR, providing direct control
381 over the expression of *khc73*.
382

eNeuro Accepted Manuscript

We obtained a third line of evidence supporting this conclusion by analyzing Khc73 expression *in vivo*. We employed HA-tagged, *khc73* transgenes with or without the 2.9kb 3'UTR along with *miR-92aSP* and quantified expression by immunohistochemistry (Figure 6D). The *UAS-HA-khc73* transgene carrying only an SV40 3'UTR exhibited robust expression in MBn using *R13F02-GAL4* (Figure 6D, left panel). Importantly, the expression was dramatically reduced when the transgene carried the *khc73* 3'UTR (Figure 6D, middle panel). This observation is consistent with the behavioral data presented above (Figure 6B). When we inhibited *miR-92a* using *miR-92aSP* transgene, we observed a low but significant level of expression (Figure 6D); supporting the conclusion that *miR-92a* represses *khc73* through its 3'UTR in vivo. Thus, the behavioral, luciferase reporter experiments and *in vivo* immunohistochemistry all support the conclusion that the *khc-73 3'UTR* provides a target for *miR-92a* repression.

DISCUSSION

MicroRNAs provide impressive regulatory power over gene expression. Individual miRNAs can repress hundreds of mRNAs simultaneously to fine tune the expression of collections of genes post-transcriptionally to regulate biological processes from early development to adult physiology. They function as gene expression rheostats that quickly respond to changing environmental conditions or developmental programs (Ferrante and Conti, 2017). In addition, the expression of miRNAs is altered under circumstances such as stress or disease states. Indeed, miRNAs are widely used as biomarkers for certain diseases and psychiatric conditions and help health care providers in diagnosis of illnesses and in judging efficacy of treatment regimens (Ridolfi

eNeuro Accepted Manuscript

406 and Abdel-Haq, 2017; Lopez et al., 2018). As previously noted, one of the earliest
407 cancer biomarkers identified was the human *miR-17-92* cluster of microRNAs (He et al.,
408 2005), for which *miR-92a* is a member. *miR-92a* has known roles in nervous system
409 development (Bian et al., 2013; Yuva-Aydemir et al., 2015); adult homeostatic synaptic
410 scaling (Letellier et al., 2014) and neuronal excitability (Chen and Rosbash, 2017).
411 Recently, *miR-92a* has been identified as a potential plasma biomarker for Alzheimer's
412 patients along with two other miRNAs (Siedlecki-Wullich et al., 2019) making *miR-92a*
413 as a notable molecule for further study in memory formation, cognition and disease.
414
415 Our data identify a new function of this conserved miRNA in *Drosophila* memory
416 consolidation, extending our knowledge of nervous system functions for *miR-92a*
417 several ways*:* (1) *miR-92a* is a memory suppressor gene, functioning in this capacity
418 specifically in the αβ and γ MBn. (2) *miR-92a* suppresses a specific process in memory
419 formation – the consolidation of early and labile memory into ARM. (3) The memory
420 suppression effect of *miR-92a* appears to occur from effects during development and
421 during adulthood. One caveat of this provisional conclusion is that the lipophilic nature
422 of the Gene-Switch inducer, RU486, may lead to its storage in fat tissues and
423 subsequent release in adult animals to maintain *miR-92aSP* expression (Mao et al.,
424 2004). (4) The memory suppressor functions of *miRNA-92a* are mediated largely by the
425 inhibition of the anterograde motor protein, Khc73. (5) *khc73,* itself, functions in the
426 same αβ and γ MBn as *miR-92a* and apparently during both development and
427 adulthood but with opposite effects: promoting consolidation rather than suppressing it.
428

eNeuro Accepted Manuscript

miR-92a function is very distinct from another suppressor, _miR-980_

MiR-92a is not the first identified memory suppressor miRNA. We previously reported that *miR-980* functions as a miRNA memory suppressor gene (Busto et al., 2015; Guven-Ozkan et al., 2016). Our findings reveal a diversity of ways by which memory suppressing miRNAs can function. *miR-980* suppresses memory broadly from functions in many different cell types in the olfactory nervous system, rather than the two types of MBn identified for *miR-92a*. This can be explained by the more general function of *miR-980*: it works by inhibiting the excitable state of neurons, setting a higher threshold for excitation and memory acquisition, rather than suppressing memory consolidation by inhibiting kinesin mediated transport functions as suggested by our current data for *miR-92a*. Moreover, the functions of *miR-980* occur during adulthood, rather than having effects during both development and adulthood as suggested by the Gene-Switch experiments with *miR-92a*. This latter observation is peculiar and poorly understood. It is possible that *miR-92a* participates in developmental processes from its developmental expression and physiological processes from adult expression. If so, the mRNA targets for *miR-92a* during development and adulthood could be similar or completely distinct, although the final developmental and adult effects on olfactory memory map to the same αβ and γ MBn.

Khc73 may be the primary target for consolidation effects

Given the large number of mRNA targets predicted for any given miRNA and the pleasing concept that miRNAs function to control the expression of groups of genes, it is surprising that our data reveal that the *miR-92a* behavioral effects can largely be

eNeuro Accepted Manuscript

452 explained by the actions of a single target, *khc73*. However, it may be that different
453 physiological or developmental events regulated by miRNAs are in some cases effected
454 by large groups of genes and others by single or small set of gene targets. In addition,
455 for miRNAs implicated in diverse physiological events, it seems likely that the mRNA
456 targets will be distinct according to the event and the cell types that are involved.
457 Moreover, although the *khc73* overexpression memory phenotypes we observed can
458 explain the *miR-92a* inhibition phenotypes, we cannot exclude the possibility that there
459 may be additional genes regulated by *miR-92a* that function in memory formation.
460 Furthermore, the *khc73* 3'UTR harbors predicted sites for other miRNAs. Tsurudome et
461 al. (2010) demonstrated that *miR-310* controls *khc73* expression at NMJ, distinct from
462 the *miR-92a* effects in MBn. Thus, this molecular motor protein is regulated by multiple
463 miRNAs in different cell types.
464
465 **Model for *miR-92a* and *khc73* function in MBn for suppression of consolidation**
466 Our data indicate that *miR-92a* suppresses memory consolidation by restricting the
467 expression of *khc73* in the αβ and γ MBn. Given the role of Kinesin-3 type motor
468 proteins in transport, along with prior studies showing that increased Khc73 expression
469 elevates synaptic transmission (Tsurudome et al., 2010), we propose that upregulated
470 Khc73 levels in *miR-92a* inhibited flies increases axonal transport and subsequent
471 neurite function and synaptic transmission. Support for this model is found from studies
472 in other systems. Puthanveettil et al (2008) showed that stimuli leading to consolidated
473 long-term facilitation of the sensory:motor neuron synapse of Aplysia require increased
474 expression of kinesin heavy chain in both pre- and post-synaptic neurons, and that

eNeuro Accepted Manuscript

upregulation of kinesin heavy chain in presynaptic neurons is sufficient for the induction of long-term facilitation. These observations, and ours, support the concept that long-term, or more generally “consolidated plasticity”, requires increased kinesin-mediated transport. Our immunohistochemistry experiments reveal that the level of Khc73 when overexpressed with its cognate 3’UTR is surprisingly low compared to when a substitute 3’UTR is utilized. This suggests that *khc73* expression is under tight post-transcriptional control through miRNA regulation. Interestingly, dimerization facilitates fast, processive movement of Khc73 along microtubules (Huckaba et al., 2011). Therefore, the level of Khc73, as regulated by *miR-92a*, may be the rate-limiting step for fast motor complexes to form. Increased Khc73 levels, due to environmental factors, developmental programs, or other elements that influence *miR-92a* function would release the brake on cargo transport leading to higher neuronal function and performance.

Our analysis pipeline for identifying *miR-92a* mRNA targets, in which we used human conservation as a criterion, identified five genes. There are *miR-92a* seed matches in human *Kif13b*, which is homologous to *Drosophila khc73*, two with identical six base pair matches in the coding sequence and one with a 5/6 base pair match in the 3’UTR. It would be interesting to test whether mammalian *miR-92a* might be involved in memory processes by regulating *Kif13b* or kinesin genes highly related to *Kif13b*. Another broad issue for future investigation surrounds the identity of other molecules that may function with *miR-92a* and *khc73* in ARM consolidation. Interestingly, the phenotypes we observed for *miR-92a* knockdown have an intriguing relationship to those for knockout of the type 2 dopamine receptor, *D2R.* The *D2R* receptor and *miR-*

eNeuro Accepted Manuscript

498 *92a* are both involved in ARM consolidation in the same MB subtypes (Scholz-Kornehl
499 and Schwarzel, 2016), with *D2R* knockout impairing memory while *miR-92a* inhibition
500 enhances memory. We tested for possible genetic interactions by epistasis
501 experiments. The memory enhancement of *miR-92a+/-* mutants was abolished and
502 indistinguishable from *D2R-/-* mutants when we tested the double mutants (Figure 7)
503 suggesting a possible genetic interaction. It would be interesting to explore the
504 mechanistic details of how *miR-92a* mediated memory enhancement is dependent on
505 dopamine signaling in the future.
506

507 **DECLARATION OF INTERESTS**

508 The authors declare no competing interests.
509

510 **REFERENCES**

511 Beck, C.D., Schroeder, B., and Davis, R.L. (2000). Learning performance of normal and
512 mutant Drosophila after repeated conditioning trials with discrete stimuli. J Neurosci *20*,
513 2944-2953.
514

515 Bian, S., Hong, J., Li, Q., Schebelle, L., Pollock, A., Knauss, J.L., Garg, V., and Sun, T.
516 (2013). MicroRNA cluster miR-17-92 regulates neural stem cell expansion and transition
517 to intermediate progenitors in the developing mouse neocortex. Cell Rep *3*, 1398-1406.
518

eNeuro Accepted Manuscript

519 Busto, G.U., Guven-Ozkan, T., Chakraborty, M., and Davis, R.L. (2016). Developmental
520 inhibition of miR-iab8-3p disrupts mushroom body neuron structure and adult learning
521 ability. Dev Biol *419*, 237-249.
522
523 Busto, G.U., Guven-Ozkan, T., and Davis, R.L. (2017). MicroRNA function in Drosophila
524 memory formation. Curr Opin Neurobiol *43*, 15-24.
525
526 Busto, G.U., Guven-Ozkan, T., Fulga, T.A., Van Vactor, D., and Davis, R.L. (2015).
527 microRNAs That Promote or Inhibit Memory Formation in Drosophila melanogaster.
528 Genetics *200*, 569-580.
529
530 Cervantes-Sandoval, I., Chakraborty, M., MacMullen, C., and Davis, R.L. (2016).
531 Scribble Scaffolds a Signalosome for Active Forgetting. Neuron *90*, 1230-1242.
532
533 Chen, X., and Rosbash, M. (2017). MicroRNA-92a is a circadian modulator of neuronal
534 excitability in Drosophila. Nat Commun *8*, 14707.
535
536 Crittenden JR, Skoulakis EM, Han KA, Kalderon D, Davis RL. (1998). Tripartite
537 mushroom body architecture revealed by antigenic markers. Learn Mem 5, 38–51.
538
539 Dietzl, G., Chen, D., Schnorrer, F., Su, K.C., Barinova, Y., Fellner, M., Gasser, B.,
540 Kinsey, K., Oppel, S., Scheiblauer, S.*, et al.* (2007). A genome-wide transgenic RNAi
541 library for conditional gene inactivation in Drosophila. Nature *448*, 151-156.

eNeuro Accepted Manuscript

Ferrante, M., and Conti, G.O. (2017). Environment and Neurodegenerative Diseases: An Update on miRNA Role. Microrna *6*, 157-165.

Fulga, T.A ., McNeill, E.M., Binari, R., Yelick, J., Blanche, A., Booker, M., Steinkraus, B.R., Schnall-Levin, M., Zhao, Y., DeLuca, T.*, et al.* (2015). A transgenic resource for conditional competitive inhibition of conserved Drosophila microRNAs. Nat Commun *6*, 7279.

Guven-Ozkan, T., Busto, G.U., Schutte, S.S., Cervantes-Sandoval, I., O'Dowd, D.K., and Davis, R.L. (2016). MiR-980 Is a Memory Suppressor MicroRNA that Regulates the Autism-Susceptibility Gene A2bp1. Cell Rep *14*, 1698-1709.

Guven-Ozkan, T., and Davis, R.L. (2014). Functional neuroanatomy of Drosophila olfactory memory formation. Learn Mem *21*, 519-526.

He, L., Thomson, J.M., Hemann, M.T., Hernando-Monge, E., Mu, D., Goodson, S., Powers, S., Cordon-Cardo, C., Lowe, S.W., Hannon, G.J.*, et al.* (2005). A microRNA polycistron as a potential human oncogene. Nature *435*, 828-833.

Heisenberg, M. (2003). Mushroom body memoir: from maps to models. Nat Rev Neurosci *4*, 266-275.

eNeuro Accepted Manuscript

565 Hu, Y., Flockhart, I., Vinayagam, A., Bergwitz, C., Berger, B., Perrimon, N., and Mohr,
566 S.E. (2011). An integrative approach to ortholog prediction for disease-focused and
567 other functional studies. BMC Bioinformatics *12*, 357.
568
569 Huckaba, T.M., Gennerich, A., Wilhelm, J.E., Chishti, A.H., and Vale, R.D. (2011).
570 Kinesin-73 is a processive motor that localizes to Rab5-containing organelles. J Biol
571 Chem *286*, 7457-7467.
572
573 Jin, J., Kim, S.N., Liu, X., Zhang, H., Zhang, C., Seo, J.S., Kim, Y., and Sun, T. (2016).
574 miR-17-92 Cluster Regulates Adult Hippocampal Neurogenesis, Anxiety, and
575 Depression. Cell Rep *16*, 1653-1663.
576
577 Letellier, M., Elramah, S., Mondin, M., Soula, A., Penn, A., Choquet, D., Landry, M.,
578 Thoumine, O., and Favereaux, A. (2014). miR-92a regulates expression of synaptic
579 GluA1-containing AMPA receptors during homeostatic scaling. Nat Neurosci *17*, 1040-
580 1042.
581
582 Lewis, B.P., Burge, C.B., and Bartel, D.P. (2005). Conserved seed pairing, often flanked
583 by adenosines, indicates that thousands of human genes are microRNA targets. Cell
584 *120*, 15-20.
585
586 Li, H.P., Liu, Z.M., and Nirenberg, M. (1997). Kinesin-73 in the nervous system of
587 Drosophila embryos. Proc Natl Acad Sci U S A *94*, 1086-1091.

eNeuro Accepted Manuscript

588

589 Lopez, J.P., Kos, A., and Turecki, G. (2018). Major depression and its treatment:
590 microRNAs as peripheral biomarkers of diagnosis and treatment response. Curr Opin
591 Psychiatry *31*, 7-16.

592

593 Loya, C.M., Lu, C.S., Van Vactor, D., and Fulga, T.A. (2009). Transgenic microRNA
594 inhibition with spatiotemporal specificity in intact organisms. Nat Methods *6*, 897-903.

595

596 Mao, Z., Roman, G., Zong, L., and Davis, R.L. (2004). Pharmacogenetic rescue in time
597 and space of the rutabaga memory impairment by using Gene-Switch. Proc Natl Acad
598 Sci U S A *101*, 198-203.

599

600 McGuire, S.E., Mao, Z., and Davis, R.L. (2004). Spatiotemporal gene expression
601 targeting with the TARGET and gene-switch systems in Drosophila. Sci STKE *2004*,
602 pl6.

603

604 Miura, P., Sanfilippo, P., Shenker, S., and Lai, E.C. (2014). Alternative polyadenylation
605 in the nervous system: to what lengths will 3' UTR extensions take us? Bioessays *36*,
606 766-777.

607

608 Mogilyansky, E., and Rigoutsos, I. (2013). The miR-17/92 cluster: a comprehensive
609 update on its genomics, genetics, functions and increasingly important and numerous
610 roles in health and disease. Cell Death Differ *20*, 1603-1614.

eNeuro Accepted Manuscript

Paraskevopoulou, M.D., Georgakilas, G., Kostoulas, N., Vlachos, I.S., Vergoulis, T., Reczko, M., Filippidis, C., Dalamagas, T., and Hatzigeorgiou, A.G. (2013). DIANA-microT web server v5.0: service integration into miRNA functional analysis workflows. Nucleic Acids Res *41*, W169-173.

Puthanveettil, S.V., Monje, F.J., Miniaci, M.C., Choi, Y.B., Karl, K.A., Khandros, E., Gawinowicz, M.A., Sheetz, M.P., and Kandel, E.R. (2008). A new component in synaptic plasticity: upregulation of kinesin in the neurons of the gill-withdrawal reflex. Cell *135*, 960-973.

Quinn, W.G., and Dudai, Y. (1976). Memory phases in Drosophila. Nature *262*, 576-577.

Ridolfi, B., and Abdel-Haq, H. (2017). Neurodegenerative Disorders Treatment: The MicroRNA Role. Curr Gene Ther *17*, 327-363.

Ruby, J.G., Stark, A., Johnston, W.K., Kellis, M., Bartel, D.P., and Lai, E.C. (2007). Evolution, biogenesis, expression, and target predictions of a substantially expanded set of Drosophila microRNAs. Genome Res *17*, 1850-1864.

Sakai, A., Saitow, F., Maruyama, M., Miyake, N., Miyake, K., Shimada, T., Okada, T., and Suzuki, H. (2017). MicroRNA cluster miR-17-92 regulates multiple functionally

eNeuro Accepted Manuscript

related voltage-gated potassium channels in chronic neuropathic pain. Nat Commun *8*, 16079.

Scholz-Kornehl, S., and Schwarzel, M. (2016). Circuit Analysis of a Drosophila Dopamine Type 2 Receptor That Supports Anesthesia-Resistant Memory. J Neurosci *36*, 7936-7945.

Siedlecki-Wullich, D., Català-Solsona, J., Fábregas, C., Hernández, I., Clarimon, J., Lleó, A., Boada, M., Saura, C.A., Rodríguez-Álvarez, J., and Alfredo J. Miñano-Molina, A.J. (2019). Altered microRNAs related to synaptic function as potential plasma biomarkers for Alzheimer's Disease. Alzheimer's Res Ther 11, 46.

Siegrist, S.E., and Doe, C.Q. (2005). Microtubule-induced Pins/Galphai cortical polarity in Drosophila neuroblasts. Cell *123*, 1323-1335.

Tempel, B.L., Bonini, N., Dawson, D.R., and Quinn, W.G. (1983). Reward learning in normal and mutant Drosophila. Proc Natl Acad Sci U S A *80*, 1482-1486.

Tsurudome, K., Tsang, K., Liao, E.H., Ball, R., Penney, J., Yang, J.S., Elazzouzi, F., He, T., Chishti, A., Lnenicka, G.*, et al.* (2010). The Drosophila miR-310 cluster negatively regulates synaptic strength at the neuromuscular junction. Neuron *68*, 879-893.

eNeuro Accepted Manuscript

Xiao, F., Zuo, Z., Cai, G., Kang, S., Gao, X., and Li, T. (2009). miRecords: an integrated resource for microRNA-target interactions. Nucleic Acids Res *37*, D105-110.

Yuva-Aydemir, Y., Xu, X.L., Aydemir, O., Gascon, E., Sayin, S., Zhou, W., Hong, Y., and Gao, F.B. (2015). Downregulation of the Host Gene jigr1 by miR-92 Is Essential for Neuroblast Self-Renewal in Drosophila. PLoS Genet *11*, e1005264.

Zhang, Y., Ueno, Y., Liu, X.S., Buller, B., Wang, X., Chopp, M., and Zhang, Z.G. (2013). The MicroRNA-17-92 cluster enhances axonal outgrowth in embryonic cortical neurons. J Neurosci *33*, 6885-6894.

FIGURE LEGENDS

Figure 1. *MiR-92a* inhibition enhances 3h olfactory memory

(A) *MiR-92a* sponge expression enhances 3h aversive memory. Pan-neuronal inhibition of *miR-92a* by expressing a *UAS-miR-92a sponge (UAS-miR-92aSP)* transgene enhances 3h memory. The *UAS-scrambled* transgene was used as the control. PI: performance index, PIs are the mean ± standard error of the mean (SEM) with n=20. Two-tailed, two-sample Student t-test, *p<0.05.

(B) *MiR-92a* heterozygous flies exhibit enhanced memory performance. Two lines of a *miR-92a* deficiency exhibit enhanced PIs compared to a *wCS10* control. PIs are the mean ± SEM with n=10. One-way ANOVA followed by Dunnett's *post-hoc* tests, *p<0.05, **p<0.01.

eNeuro Accepted Manuscript

679 **Figure 2. Memory enhancement from inhibiting *miR-92a* in mushroom body neurons**

680 (A) *MiR-92a* inhibition in mushroom bodies enhances 3h memory. The *UAS-scrambled* and
681 *UAS-miR-92aSP* flies were crossed to a battery of *GAL4* lines that drive expression in specific
682 populations of neurons. Most of the drivers promote expression in neurons of the olfactory
683 pathway. The *GAL4* drivers used and abbreviations of their expression domains are shown
684 below the bar graph. Note that there is some variation in the scores of the control genotypes
685 due to using different *GAL4* drivers. Pn: projection neurons, APLn: anterior paired lateral
686 neuron, MBn: mushroom body neurons, DPMn: dorsal paired medial neuron, CC: central
687 complex, DAn: dopaminergic neurons, In: inhibitory neurons. PIs are the mean ± SEM with
688 n=12. Two-tailed, two-sample Student's t-tests for each driver expressing *miR-92aSP*
689 compared with expression of the scrambled control, *p<0.05.

690 (B) *MiR-92a* spatial mapping to subsets of mushroom body neurons. Two independent
691 drivers were used for each type of mushroom body neuron: α'β', γ and αβ. The *GAL4* drivers
692 employed and their expression in the three broad types of mushroom body neurons are shown
693 below the graph. PIs are the mean ± SEM with n=12. Two-tailed, two-sample Student's t-tests
694 for each driver expressing *miR-92aSP* compared with expression of the scrambled control,
695 *p<0.05, **p<0.01

696 (C) Overexpression of *miR-92a* does not affect 3h memory. *MiR-92a* was overexpressed in
697 αβ and γ mushroom body neurons using *R25H11-GAL4*. Three hr olfactory memory
698 performance of *R25H11-GAL4>UAS-miR-92a* flies was compared to *GAL4*-only and *UAS*-only
699 controls. PIs are the mean ± SEM with n=14. One-way ANOVA followed by Bonferroni's *post-*
700 *hoc* tests. *n.s.,* not significant.

eNeuro Accepted Manuscript

(D) Memory enhancement occurs from *miR-92a* inhibition during both development and adulthood as assayed using the Gene Switch System. Administration of RU486 during development (*devel*), adulthood (*adult*), or both (*devel* + *adult*) modulates mushroom body expression of *miR-92aSP* controlled by the MB-Gene-Switch driver. Note that RU treatment either during development or adulthood alters the PIs of the control genotype. PIs are the mean ± SEM with n=6-8. Two-tailed, two-sample Student's t-tests for each RU486 feeding condition, *p<0.05, ***p<0.001.

Figure 3. Inhibiting *miR-92a* enhances intermediate term memory

(A) Memory decay in flies expressing *miR-92aSP* in the mushroom bodies. Three min, 1, 2, 3, 6 and 9h memory was tested in flies expressing *UAS-miR-92aSP* or *UAS-scrambled* under the control of *R13F02-GAL4*. PIs are the mean ± SEM with n=6-8. Two-tailed, two-sample Student's t-tests between the groups at each time point, *p<0.05.

(B) No effect of *miR-92a* inhibition on memory acquisition. Three min memory of *R13F02-GAL4>UAS-scrambled* or *R13F02-GAL4>UAS-miR-92aSP* flies tested after 1, 2, 3, 4, 6 and 12 shock-training paradigms. PIs are the mean ± SEM with n=6. Two-tailed, two-sample Student's t-tests for each shock group of flies expressing *miR-92aSP* compared with expression of the scrambled control. No significant differences were found.

Figure 4. Inhibiting *miR-92a* enhances memory consolidation

(A) Three-hour memory performance of *R25H11-GAL4>UAS-scrambled* or *R25H11-GAL4>UAS-miR-92aSP* flies with or without cold shock induced amnesia applied 2h after aversive training. Cold-shocked flies exhibited increased performance, indicating enhanced

eNeuro Accepted Manuscript

724 ARM. PIs are the mean ± SEM with n=14-16. Two-tailed, two-sample Student's t-tests,
725 *p<0.05.
726 (B) Three-hour memory performance of *R25H11-GAL4>UAS-scrambled* or *R25H11-*
727 *GAL4>UAS-miR-92aSP* flies subjected to cold shock induced amnesia at various time points
728 after aversive training. PIs are the mean ± SEM with n=12-16. Two-tailed, two-sample
729 Student's t-tests, *p<0.05.
730
731 **Figure 5. *MiR-92a* mRNA target prediction**
732 (A) Design of the mRNA target prediction pipeline. Top predictions for DIANA and
733 TargetScan have 11 genes in common, 6 of which are also predicted by miRecords. Five of
734 these potential mRNA targets have human homologs that are predicted targets for human
735 *miR-92a*.
736 (B) *khc73 RNAi* expression produces memory impairment. Only *khc73* of the 5 candidates
737 (Table S1) significantly impaired 3h memory using RNAi driven by pan-neuronal *nSyb-GAL4*.
738 PIs are the mean ± SEM with n=10. Two-tailed, two-sample Student's t-tests, *p<0.05.
739 (C) *UAS-khc73* overexpression enhances 3h memory. Expression of *UAS-khc73* driven by
740 *R25H11-GAL4* significantly enhanced 3h memory compared to *UAS*-only and *GAL4*-only
741 controls. PIs are the mean ± SEM with n=10. One-way ANOVA followed by Bonferroni's *post-*
742 *hoc* tests, *p<0.05, **p<0.01.
743 (D) Overexpressing *khc73* using *R25H11-GAL4* enhances ARM. Flies were subjected to
744 cold shock 2h after aversive conditioning and memory was tested at 3h. Consistent with *miR-*
745 *92a* inhibition, overexpressing *khc73* enhances ARM. PIs are the mean ± SEM with n=12.
746 Two-tailed, two-sample Student's t-tests, *p<0.05, ***p<0.001.

eNeuro Accepted Manuscript

747 (E) Overexpressing *khc73* during development (*devel*), adulthood (*adult*), or both (*devel+*
748 *adult*) enhances adult memory as assayed using the Gene Switch System. Administration of
749 RU486 increases mushroom body expression of *khc73* controlled by the MB-Gene-Switch
750 driver. Similar to the effect observed in Figure 2D, RU treatment either during development or
751 adulthood alters the PIs of the control genotype. PIs are the mean ± SEM with n=16-20. Two-
752 tailed, two-sample Student's t-tests for each RU486 feeding condition, *p<0.05.
753
754 **Figure 6. Memory performance of flies overexpressing *khc73* with and without the**
755 **endogenous 3'UTR**
756 (A) Three predicted *miR-92a* binding sites in the endogenous 3'UTR are schematized.
757 Renilla luciferase reporter was cloned upstream of the 2.7kb *khc73 3'UTR* and used for the
758 experiment shown in Figure 6C. Nucleotides with predicted *miR-92a* binding are shown in red
759 font. All three *miR-92a* sites were altered to generate a mutant *khc73 3'UTR* that is
760 unresponsive to *miR-92a* repression (shown with orange font) as a negative control for
761 luciferase experiments.
762 (B) Overexpressing *khc73* with the endogenous 3'UTR eliminates the memory
763 enhancement gained without the 3'UTR. Expression of HA-tagged *khc73* transgenes with or
764 without 2.9kb of its own 3'UTR confers normal and enhanced memory performance,
765 respectively. PIs are the mean ± SEM with n=14. One-way ANOVA followed by Bonferroni's
766 *post-hoc* tests, *p<0.05, ***p<0.001.
767 (C) Overexpressing *miR-92a* represses expression of a *khc73 3'UTR* luciferase reporter.
768 The Renilla luciferase signal was normalized to Firefly luciferase for each transfection.
769 *C.elegans miR-239b* served as negative and *Drosophila miR-310* as positive controls.

eNeuro Accepted Manuscript

770 Renilla/Firefly ratios were normalized to negative controls for each reporter construct. Relative
771 repression ratios ± SEM with n=9. One-way ANOVA followed by Bonferroni's *post-hoc* tests,
772 ***p<0.001. wt: wild type.
773 (D) *miR-92a* inhibition derepresses HA-Khc73 signal. HA-Khc73 transgenes with or without
774 the endogenous 2.9kb 3'UTR element were overexpressed in MBn using the *R13F02-GAL4*
775 driver. The presence of the endogenous 3'UTR constraints the HA-Khc73 signal. Very weak
776 signals in the mushroom bodies were detected (middle column) and quantified (bar plot). This
777 weak signal was significantly derepressed when the *miR-92aSP* was co-expressed (right
778 column). The bar plot shows the quantification of *R13F02>scrambled*, *HA-khc73+3'UTR*
779 versus *R13F02>miR-92aSP, HA-khc73+3'UTR* brains. ROI was taken from the horizontal
780 lobes by reference to anti-Scribble signal. HA/Scribble ratios were used to minimalize brain to
781 brain variability. Ratios are the mean ± SEM with n=26-30. Two-tailed, two-sample Student's t-
782 tests, *p<0.05.
783
784 **Figure 7. Memory enhancement of *miR-92a+/-* mutant flies requires *D2R,* type 2**
785 **dopamine receptor**
786 Three-hour memory scores of *miR-92a+/-, D2R-/-* and *D2R-/-; miR-92a+/-* double mutants
787 were tested and compared to *wCS10* control using one-way ANOVA followed by Bonferroni's
788 *post-hoc* tests, *p<0.05, **p<0.01, ***p<0.001. PIs are the mean ± SEM with n=20-23.
789
790 **EXTENDED DATA**
791 **Figure 1-1. Odor and shock avoidance of *miR-92aSP*-expressing and *miR-92a***
792 **heterozygous flies**

eNeuro Accepted Manuscript

793 (A) The *c155-GAL4>UAS-miR-92aSP* flies avoided ben, oct and electric shock stimuli
794 indistinguishably from *c155>UAS-scrambled* flies. Avoidance Index: AI, AI's are the mean ±
795 SEM with n=6. Two-tailed, two-sample Student's t-tests for each condition. No significant
796 differences were detected.
797 (B) *miR-92a* heterozygotes for Clones D and N flies avoided ben, oct and electric shock
798 stimuli indistinguishably from the *wCS10* control. AI's are the mean ± SEM with n=6. Two-
799 tailed, two-sample Student's t-tests for each condition. No significant differences were
800 detected.
801
802 **Figure 2-1. Odor and shock avoidance of *miR-92aSP* and *khc73* overexpression flies**
803 (A,B,C,D) Flies carrying *UAS-miR-92aSP* driven by *R13F02-GAL4, R11D09-GAL4,*
804 *R28H05-GAL4, or R25H11-GAL4* avoided ben, oct and electric shock stimuli indistinguishably
805 from flies carrying *UAS-scrambled* and the same drivers. AI's are the mean ± SEM with n=6.
806 Two-tailed, two-sample Student's t-tests for each condition. No significant differences were
807 detected.
808 (E) *R25H11-GAL4>UAS-khc73* animals avoided ben and oct indistinguishably from *GAL4-*
809 only and UAS-only controls. The *UAS-khc73/+* control group exhibited an increased avoidance
810 of shock stimuli compared to the *R25H11/+* control and *R25H11-GAL4>UAS-khc73*
811 experimental flies. This increased avoidance fails to explain the memory enhancement of the
812 experimental genotype. AI's are the mean ± SEM with n=6. One-way ANOVA followed by
813 Bonferroni's *post-hoc* tests, *p<0.05.
814
815 **Figure 3-1. *MiR-92aSP* memory retention, acquisition and cold shock experiments with**
816 **mushroom body γ and αβ drivers**

eNeuro Accepted Manuscript

817 (A) *miR-92a* inhibition enhances intermediate-term memory. Inhibiting *miR-92a* in γ
818 mushroom body neurons using *R11D09-GAL4* enhances 1h and 3h memory. Inhibiting *miR-*
819 *92a* in αβ mushroom body neurons using the *R28H05-GAL4* driver enhances 1h, 3h and 6h
820 memory. The PI for *UAS-miR-92aSP*-expressing flies was compared to the PI for *UAS-*
821 *scrambled*-expressing flies at each time point. PIs are the mean ± SEM with n=12. Two-tailed,
822 two-sample Student's t-tests for each time point, *p<0.05, **p<0.01.
823 (B) *miR-92a* inhibition does not affect acquisition. Three min memory of *R11D09-GAL4* or
824 *R28H05-GAL4* driven *miR-92aSP* flies tested after receiving varying numbers of shock pulses
825 with a 1min CS+ odor presentation. PIs are the mean ± SEM with n=6-12. Two-tailed, two-
826 sample Student's t-tests. No significant differences were detected.
827 (C) Inhibiting *miR-92a* in γ and αβ mushroom body neurons enhances ARM. Flies were
828 subjected to cold shock 2h after aversive conditioning and memory was tested at 3h. Memory
829 of *R11D09-GAL4* and *R28H05-GAL4* driven *miR-92aSP* flies was tested with or without cold
830 shock treatment. PIs are the mean ± SEM with n=16-20. Two-tailed, two-sample Student's t-
831 tests, *p<0.05, **p<0.01.
832
833
834

eNeuro Accepted Manuscript

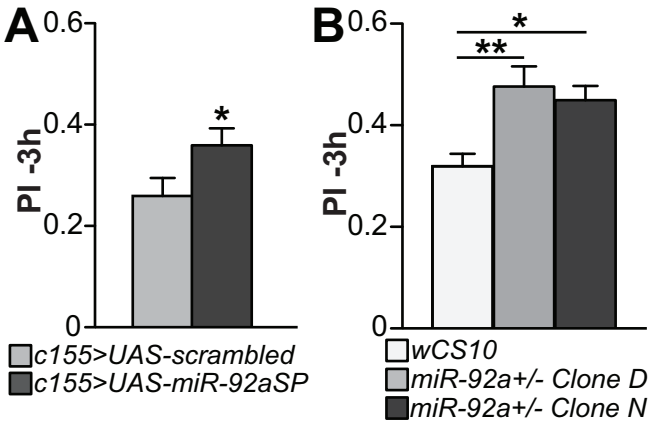

eNeuro Accepted Manuscript

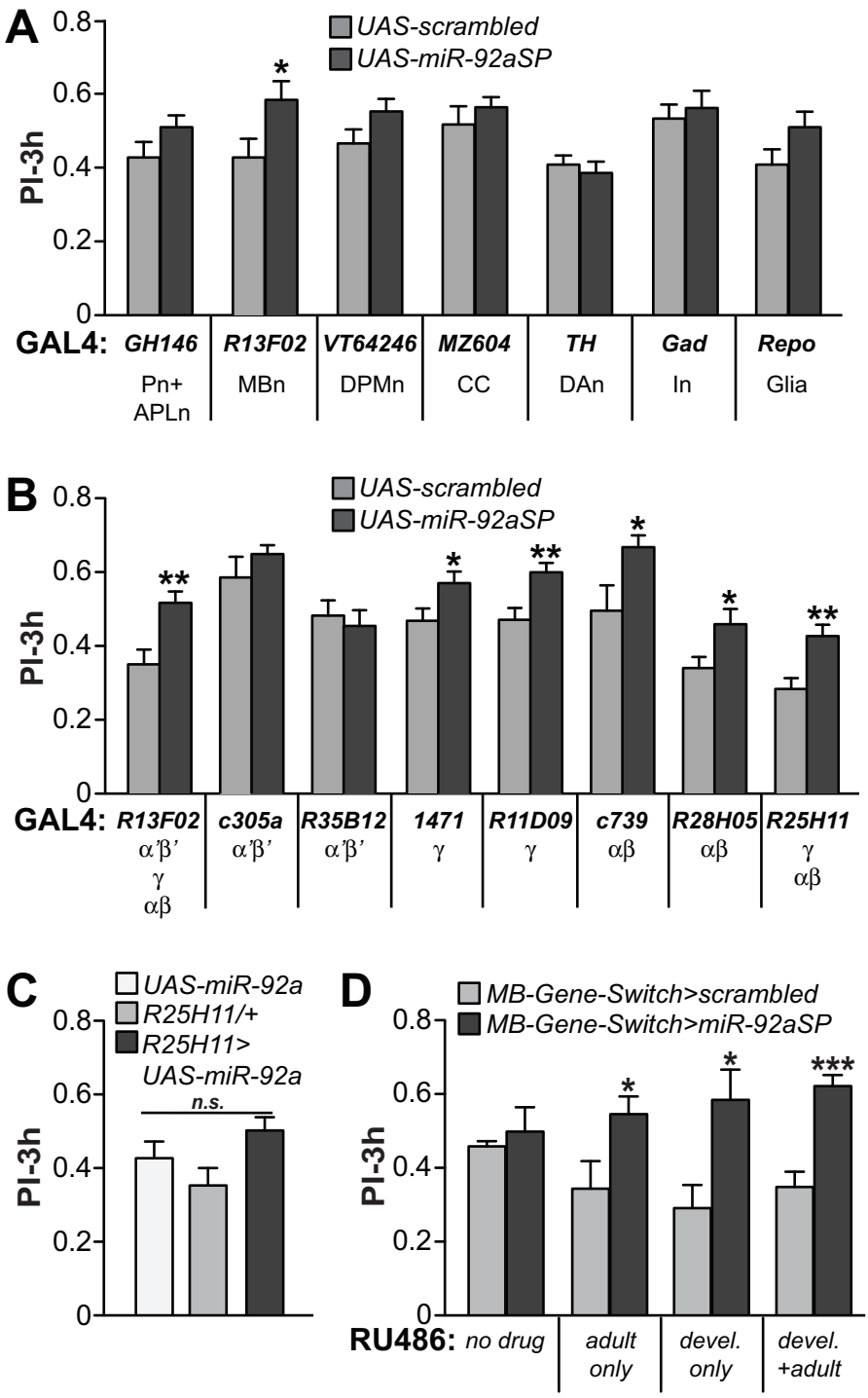

eNeuro Accepted Manuscript

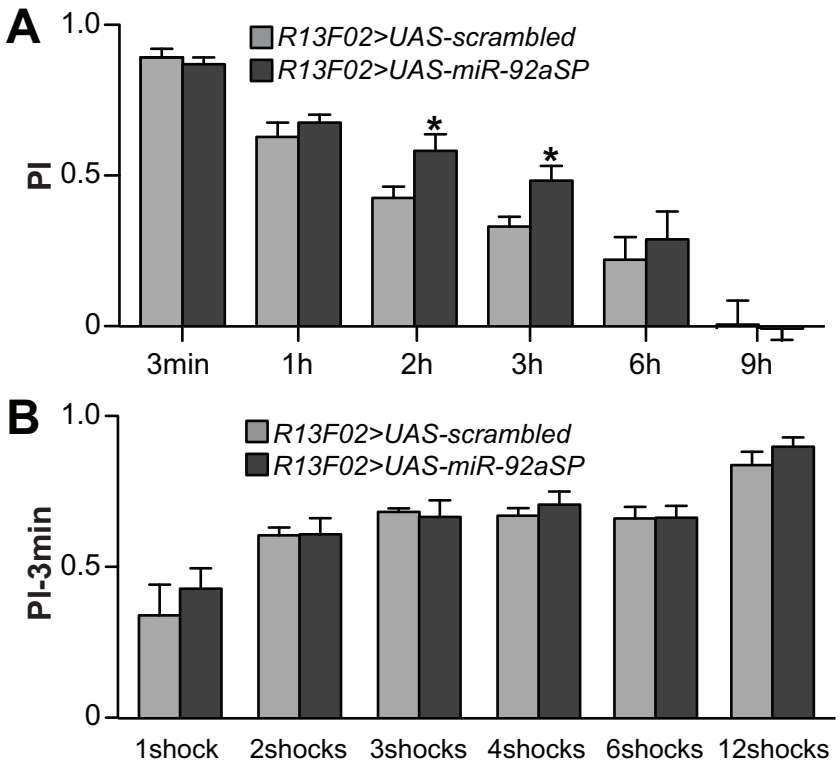

eNeuro Accepted Manuscript

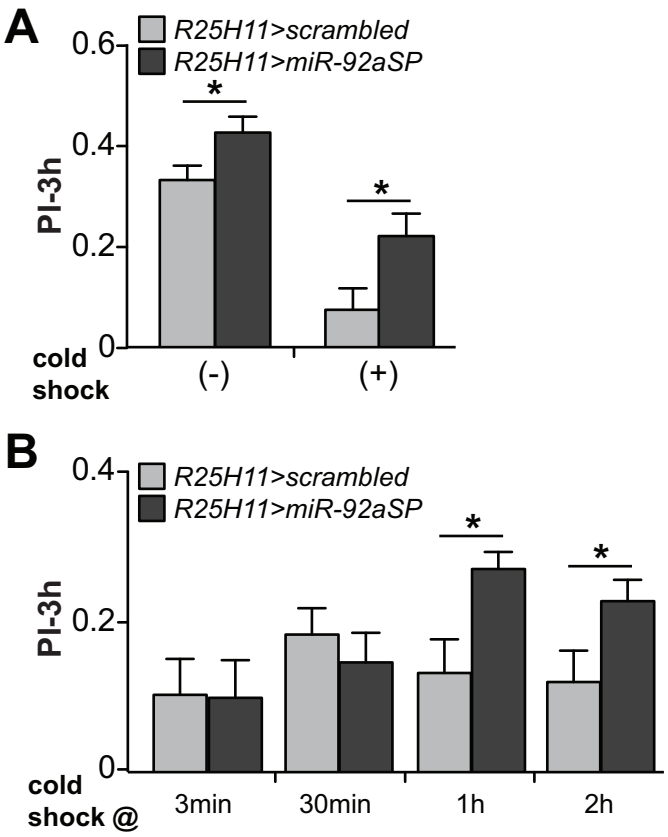

eNeuro Accepted Manuscript

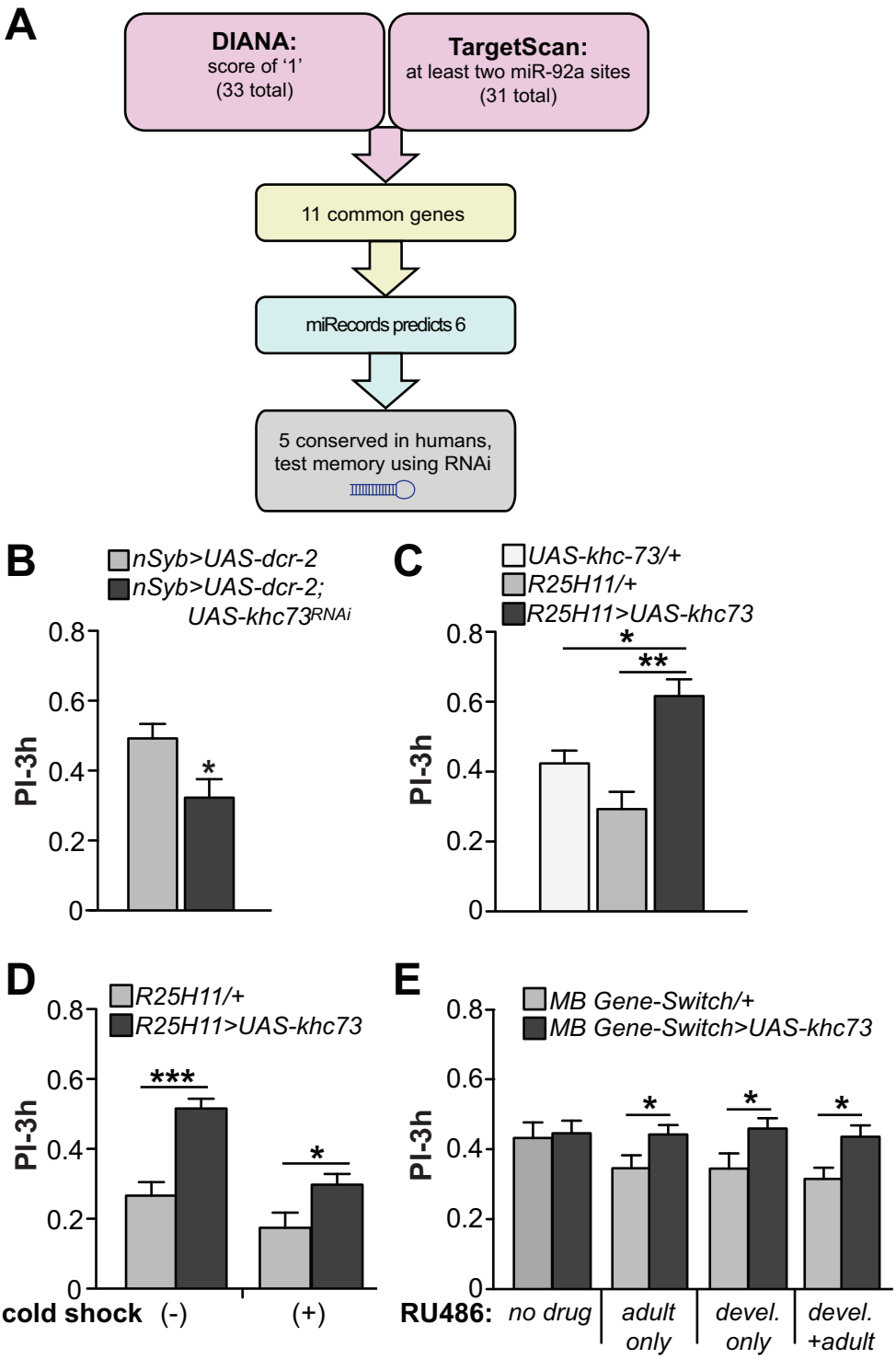

eNeuro Accepted Manuscript

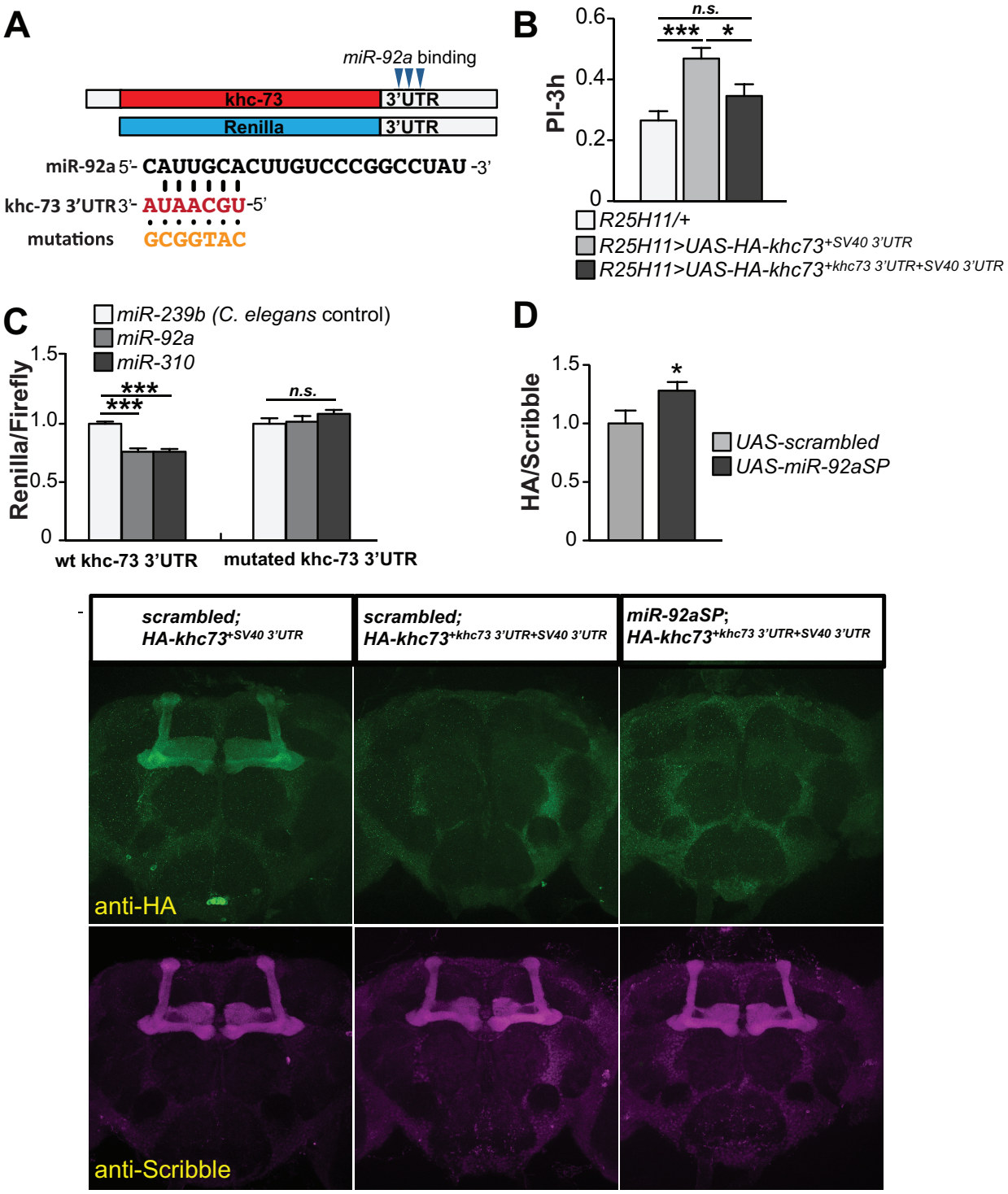

eNeuro Accepted Manuscript

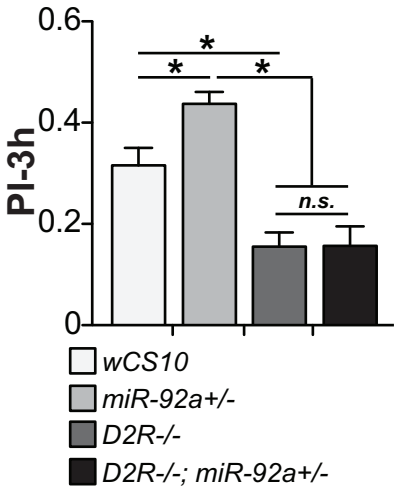

eNeuro Accepted Manuscript

Table 1. Putative *miR-92a* Target Genes

Gene Name	Flybase ID	RNAi line	PI for *nSyb-GAL4* screen	Retest score	p value
CG12024	*CG12024*	GD-20143	0.45±0.02		
CG8360	*CG8360*	GD-41643	0.40±0.08		
cpr50Ca	CG13338	KK-100317	0.64±0.07	0.56±0.08	0.15
khc-73	CG8183	KK-105984	0.38±0.09	0.28±0.07	0.02*
crebA	CG7450	KK-110650	0.37±0.06	0.37± 0.08	0.09

Candidate mRNA targets for *miR-92a* were selected by applying the pipeline described in Figure 5A. Five genes were screened for a role in memory formation using an RNAi approach. The 5 lines from the Vienna *Drosophila* RNAi Center (http://stockcenter.vdrc.at/control/main) that were tested are listed. RNAi lines were crossed to the *nSyb-GAL4* driver and tested for 3h memory with n=4. Each individual RNAi line was compared to a daily *nSyb-GAL4>UAS-dcr-2* control in the respective GD or KK background. The average performance index for the *nSyb-GAL4>UAS-dcr-2* control was 0.36±0.1 for the GD control (n=4) and 0.49±0.04 for the KK control. Three lines with a trend for a significant effect on memory were retested with n=6. Only the *khc-73* RNAi line, KK-105984 (highlighted), had a PI significantly lower than the control (n=10). Results shown are the mean ± SEM. Two-tailed, two-sample Student's t-tests.